


## Fractional Mathematical Modelling of The Spread of Rotavirus Disease

\*Fatma Özköse 

†Erciyes Üniversitesi Fen Fakültesi Matematik Bölümü, KAYSERİ

(Alınış / Received: 09.06.2023, Kabul / Accepted: 07.08.2023, Online Yayınlanma / Published Online: 31.08.2023)

### Keywords

Fractional order derivative,  
Stability,  
Numerical solutions,  
Numerical simulation,  
Existence-uniqueness

**Abstract:** In this study, rotavirus disease is examined. In this situation, many variables are used to construct a fractional mathematical model. The model is employed to determine how the disease's transmission will affect susceptible, infected, and recovered individuals. The implications of the fractional derivative on the stability and dynamic behaviour of solutions are examined using the formulation of the Caputo fractional operator. The existence and uniqueness, positivity and boundedness of the solution are next examined. Findings include equilibrium points and stability requirements.

Numerical simulations are used to examine the system's dynamic behaviour. With the use of these simulations, it is possible to study how susceptible, infected, and recovered people change over time by giving fractional values to fractional order  $\vartheta$ .  $\vartheta$  takes values in the range  $[0,1]$ . This highlights the advantages of using fractional differential equations. Then it is seen how changing some parameters causes changes in susceptible, infected and recovered individuals.

## Rotavirüs Hastalığının Yayılımının Kesirli Matematiksel Modellemesi

### Anahtar Kelimeler

Kesirli mertebeden türev,  
Kararlılık,  
Sayısal çözümler,  
Sayısal benzetimler,  
Varlık-teklik

**Öz:** Bu çalışmada rotavirüs hastalığı incelenmiştir. Bu durumda, kesirli bir matematiksel model oluşturmak için birçok değişken kullanılır. Model, hastalığın bulaşmasının duyarlı, enfekte ve iyileşmiş bireyleri nasıl etkileyeceğini belirlemek için kullanılır. Kesirli türevin çözümlerin kararlılığı ve dinamik davranışı üzerindeki etkileri, Caputo kesirli operatörünün formülasyonu kullanılarak incelenir. Daha sonra çözümün varlığı ve tekliği, pozitifliği ve sınırlılığı incelenir. Bulgular, denge noktalarını ve kararlılık gereksinimlerini içerir.

Sayısal benzetimler, sistemin dinamik davranışını incelemek için kullanılır. Bu benzetimlerin kullanımıyla,  $\vartheta$  kesirli mertebesine kesirli değerler vererek duyarlı, enfekte ve iyileşmiş insanların zaman içinde nasıl değiştiğini incelemek mümkündür.  $\vartheta$ ,  $[0,1]$  aralığında değerler alır. Bu, kesirli diferansiyel denklemleri kullanmanın avantajlarını vurgular. Daha sonra bazı parametrelerin değiştirilmesinin duyarlı, enfekte ve iyileşmiş bireylerde nasıl değişikliklere neden olduğu görülür.

\*Corresponding Author, email: fpeker@erciyes.edu.tr

## 1. Introduction

Rotaviruses are the leading cause of diarrhea in infants and young children, especially severe gastroenteritis, which causes hospitalizations and infant deaths worldwide [1]. The disease constitutes an average of 20% of all diarrhea-related deaths in the world [2]. Rotavirus is a virus that causes intestinal inflammation, especially in children under 2 years of age. The disease is manifested by severe fever, diarrhea, and vomiting. The transmission route of the disease is oral - fecal route. The disease makes epidemics, especially in winter and spring. [2, 3]. Due to rotavirus (RV) diarrhea, there are approximately twenty five million outpatient clinic applications worldwide every year, two million children are hospitalized and more than 600,000 children are lost [4]. In other words, one child is lost every minute due to RV gastroenteritis. Rotaviruses take the second place after pneumococci among vaccine-preventable disease deaths in children under five years of age [5]. Studies show that rotavirus is an important cause of gastroenteritis in children aged 0-5 years in our country [6-9]. Rotavirus diarrhea is a problem of both developed and developing countries all over the world. Rotavirus infections, which differ from other gastroenteritis agents by not being dependent on socioeconomic conditions and hygiene measures, are seen with the same frequency in developed and developing countries; while it progresses with high mortality in developing countries, it results in high morbidity and economic losses in developed countries [6,10,11]. Mızrakçı [12] and Aydın [13] conducted studies on Rotavirus. Examining the development and course of epidemic diseases is of great importance in terms of diagnosis and treatment. Mathematical models are used because there is no mechanism to completely eliminate the disease. Therefore, mathematical models have become necessary diagnostic and therapeutic tools for treatment. Since 1927, mathematical models have been extensively employed to understand the course of disease. Recently, scientists have worked on fractional differential equations when creating mathematical models. The classical concepts of derivative and integral, which Leibniz and Newton both fully investigated, are generalised by the fractional derivative and integral. Both the ideas of fractional derivative and integral are historically significant [14]. In addition to Leibniz, many mathematicians such as Weyl, Liouville, Lagrange, Riemann Laplace, Fourier, Abel and Euler have done various studies on this subject [15]. Various definitions of the fractional derivative have been made in the literature. Some of these are Caputo, Riemann-Liouville, Grünwald-Letnikov, Riesz, Wely fractional derivatives. Some studies have shown that these definitions are the same under certain conditions. Although there are transitions between them, their definitions and physical interpretations are different [16-19]. It is possible to select the derivative definition most appropriate for the type of issue at hand and so arrive at the optimum solution by using several definitions of derivatives in fractional analysis. The Caputo definition of the fractional derivative is created by the Italians. In the 1960s, the mathematician Riemann-Liouville eliminated the problem of calculating or experimentally measuring the initial values that arose in applications of the Laplace transform of the M. Caputo definition. For this reason, in some recent studies in the literature, fractional derivative operators are preferred more than Caputo and Riemann-Liouville fractional derivative operators for numerical and analytical solutions of fractional differential equations. The Caputo derivative employs fractional derivatives. Let's give examples from the studies on the mathematical modeling of some diseases in recent years employing the Caputo fractional derivative: Öztürk et al. [20] examined the stability of the fractional-order model of the tumor-immune system interaction. Naik et al. [21] created a dynamic fractional-order HIV-1 model that takes into account interactions between cancer cells, healthy lymphocytes, and lymphocytes that have been virus-infected to cause chaotic behaviour. Özköse et al. [22] used the Caputo fractional derivative to study the long-term impact of treatment on tumour cells and stem cells. Özköse et al. [23] conducted several studies on a new fractional grade model of SARS-CoV-2 and Cholera disease with real data. Yavuz et al. [24] conducted several studies on a new fractional rank and susceptibility analysis modeling for hepatitis-b disease with real data. Sabbar et al. [25] conducted various studies on the general epidemic model in their study called Logistic Growth, Quarantine Strategy, Media Attack and Quadratic Perturbation, and Infection Eradication Criteria in the General Outbreak Model. Sene et al. [26] demonstrated the theory and applications of the fractional chaotic system by using the Caputo operator in her work called Theory and Applications of the New Fractional Chaotic System Under the Caputo Operator. Evirgen et al. [27] carried out studies on the modeling of influenza disease dynamics under the Caputo-Fabrizio fractional derivative with different contact rates. Veerasha et al. [28] studied the Korteweg-De Vries equation with three fractional operators in his work A computational approach for shallow water forced the Korteweg-De Vries equation at critical flow over a hole with three fractional operators. Odionyenma et al. [29] analyzed a model using the Caputo derivative in her study Analysis of a model for controlling the joint dynamics of Chlamydia and Gonorrhoea using the Caputo fractional derivative. Atede et al. [30] studied a fractional grade vaccination model for COVID-19 involving environmental transmission: A case study using Nigerian data, using Nigerian data on a fractional grade vaccination model. Nwajeri et al. [31] examined the mathematical modeling of malaria and cholera disease with the help of fractional differential equations in her study named co-dynamic model analysis furnished with fractional differential equations of malaria and cholera. The model's formulation is described first, after which the model's existence and uniqueness are demonstrated. It has been shown that the parameters that will control the spread of the disease are determined by the fundamental reproduction number and equilibrium points. The article's sections are arranged in the following order: The most significant definitions of fractional calculus are covered in Section 2. In Section 3, we describe a fractional order

model. In Section 4, we show that the solution to this model exists and is unique. We identify the equilibrium points of the model's solution and evaluate their stability in Section 5. We find positivity and boundedness in Section 6. In Section 7, we present the numerical technique for this model. In Section 8, we utilise the parameter values from Table 1 to numerically solve our model using the Adams-Bashforth Moulton approach. Finally, Section 9 provides the conclusion.

**2. Preliminaries**

We give a few key definitions of fractional calculus [16,25] that are crucial to understanding this text in this part.

**Definition 1.** Fractional integral from order  $\vartheta$  is described as

$$I^\vartheta f(t) = \int_0^t \frac{(t-s)^{\vartheta-1}}{\Gamma(\vartheta)} f(s) ds,$$

where  $\vartheta > 0, t > 0$  and  $\Gamma$  is the Gamma function, the fractional derivative is described as

$$D^\vartheta f(t) = I^{n-\vartheta} D^n f(t) \left( D = \frac{d}{dt} \right),$$

where  $\vartheta \in (n-1, n), t > 0$ .

**Definition 2.**

$$\begin{aligned} {}_0^C D_t^\vartheta f(t) &= \frac{1}{\Gamma(n-\vartheta)} \int_0^t \frac{\left(\frac{d}{d\tau}\right)^n f(\tau)}{(t-\tau)^{\vartheta-n+1}}, & 0 \leq n-1 < \vartheta < n, & \quad n = [\vartheta], n \in \mathbb{N}, \\ & \left( \frac{d}{dt} \right)^n f(t), & \vartheta = n, n \in \mathbb{N}. \end{aligned} \tag{1}$$

gives the definition of the Caputo fractional derivative of order  $\vartheta > 0$  of  $f: (0, \infty) \rightarrow \mathcal{R}$ .

**Definition 3.** The Laplace transform (LT) of the Caputo operator of the function  $f(t)$  of order  $\vartheta > 0$  is described by

$$L[{}_0^C D_t^\vartheta f(t)] = s^\vartheta F(s) - \sum_{v=0}^{n-1} f^{(v)}(0) s^{\vartheta-v-1} f^{(v)}(0). \tag{2}$$

**Definition 4.** The Laplace transform (LT) of the function  $f(t) = t^{\vartheta_1-1} E_{\vartheta, \vartheta_1}(\pm wt^\vartheta)$  is described as

$$L[t^{\vartheta_1-1} E_{\vartheta, \vartheta_1}(\pm wt^\vartheta)] = \frac{s^{\vartheta-\vartheta_1}}{s^\vartheta \pm w}, \tag{3}$$

where  $E_{\vartheta, \vartheta_1}$  is Mittag-Leffler function.

**Definition 5.** The gamma function is defined for  $Re(z) > 0$

with the help of the integral

$$\Gamma(z) = \int_0^\infty e^{-t} t^{z-1} dt.$$

One of the gamma function's fundamental characteristics is

$$\Gamma(z + 1) = z\Gamma(z),$$

$$\Gamma(n + 1) = n!$$

for  $z \in \mathbb{C}, n \in N_0$ . The gamma function has singular poles at  $z = -n (n = 0, 1, 2, \dots)$ .

**Theorem 1** [32,33]. Consider the following fractional order system:

$$\frac{d^\vartheta X}{dt^\vartheta} = f(X), \quad X(0) = X_0, \tag{4}$$

with  $X \in \mathcal{R}^n$  and  $\vartheta \in (0, 1]$ . The equilibrium points of the system (4) are solutions to the equation  $f(X^*) = 0$ , and these equilibrium points:

- (1) Asymptotically stable  $\Leftrightarrow$  all the eigenvalues  $\lambda_i, i = 1, 2, \dots, n$  of the Jacobian matrix  $J(X^*)$  satisfy that  $|\arg(\lambda_i)| > \frac{\vartheta\pi}{2}$ .
- (2) Stable  $\Leftrightarrow$  it is asymptotically stable or the eigenvalues  $\lambda_i, i = 1, 2, \dots, n$  of  $J(X^*)$  that satisfy  $|\arg(\lambda_i)| = \frac{\vartheta\pi}{2}$  if have the same geometric multiplicity and algebraic multiplicity.
- (3) Unstable  $\Leftrightarrow$  eigenvalues  $\lambda_i$  for some  $i = 1, 2, \dots, n$  of  $J(X^*)$  satisfy  $|\arg(\lambda_i)| < \frac{\vartheta\pi}{2}$ .

### 3. Mathematical Modelling

Mathematical models can be used to forecast the occurrence and severity of viral infections. Many diseases may be treated and their spread halted using mathematical models. Our aim is to monitor the spread of the disease with the help of these mathematical models and to help science by observing the effect of this disease on people. Rotavirus disease, which has spread since 2003, has been causing the death of many people every year. To examine the spread of rotavirus, we consider three subpopulations susceptible, rotavirus-infected, and recovered.  $S$  stands for a susceptible person,  $I$  rotavirus-infected person,  $R$  the population that has recovered, and  $N$  total population. The recommended fractional order model is as follows:

$$\begin{aligned} D^\vartheta S(t) &= \Lambda - \beta_1 \frac{S(t)I(t)}{N} - \mu S(t), \\ D^\vartheta I(t) &= \beta_1 \frac{S(t)I(t)}{N} - \mu I(t) - \alpha_2 I(t) - \alpha_3 I(t), \\ D^\vartheta R(t) &= \alpha_2 I(t) - \mu R(t). \end{aligned} \tag{5}$$

with initial settings

$$S(0) = S_0 \geq 0, I(0) = I_0 \geq 0, R(0) = R_0 \geq 0.$$

The biological effects of the system (5) parameter values are presented in the following Table.

Parameters	Meaning	Value	Source
$\Lambda$	Recruitment rate	2.2996e+03	[32]
$\mu$	The natural death rate	0.0336080229	Estimated
$\alpha_2$	The rate of people recovered from the I class	0.008841	Estimated
$\alpha_3$	Death rate of disease	0.024	[33]
$\beta_1$	Rate of disease transmission	0.3736	[33]

Rotavirus disease is an infectious disease like covid 19 and shows a similar spread. SIR mathematical modeling is used in both of these diseases. Therefore, parameter values can be taken the same. The article for covid 19 is an extended version of the SIR model.

#### 4. Existence and Uniqueness

Let us assess the system (5) under its initial settings  $S(0) = S_0, I(0) = I_0, R(0) = R_0$ .

The formula for the system (5) is:

$$D^\theta X(t) = B_1 X(t) + S(t)B_2 X(t) + I(t)B_3 X(t) + V,$$

$$X(0) = X_0, \tag{6}$$

where

$$X(t) = \begin{pmatrix} S(t) \\ I(t) \\ R(t) \end{pmatrix}, X(0) = \begin{pmatrix} S(0) \\ I(0) \\ R(0) \end{pmatrix},$$

$$B_1 = \begin{pmatrix} -\mu & 0 & 0 \\ 0 & -\mu - \alpha_2 - \alpha_3 & 0 \\ 0 & \alpha_2 & -\mu \end{pmatrix}, B_2 = \begin{pmatrix} 0 & \frac{-\beta_1}{N} & 0 \\ 0 & 0 & 0 \\ 0 & 0 & 0 \end{pmatrix}, B_3 = \begin{pmatrix} 0 & 0 & 0 \\ \frac{\beta_1}{N} & 0 & 0 \\ 0 & 0 & 0 \end{pmatrix}, V = \begin{pmatrix} \Lambda \\ 0 \\ 0 \end{pmatrix}.$$

**Definition 7** [33]. Let  $C^*[0, \tau^*]$  be the class of continuous column  $X(t)$  whose components  $S, I, R \in C^*[0, \tau^*]$  are the class of continuous functions on the interval  $[0, \tau^*]$ . The norm of  $X \in C^*[0, \tau^*]$  is given by

$$\|X\| = \sup_t |e^{-Nt} S(t)| + \sup_t |e^{-Nt} I(t)| + \sup_t |e^{-Nt} R(t)|,$$

where  $N$  is a natural number and when  $t > \delta \geq m$ , we write  $C_\delta^*[0, \tau^*]$  and  $C_\delta[0, \tau^*]$ .

**Definition 8** [33].  $X \in C^*[0, \tau^*]$  is a solution of IVP (6) if

- (1)  $(t, X(t)) \in D, t \in [0, \tau^*]$  where  $D = [0, \tau^*] \times K, K = \{(S, I, R) \in \mathcal{R}_+^3: |S| \leq p, |I| \leq r, R \leq w\}$ ,  
 $p, r, w \in \mathcal{R}_+$  are constants.
- (2)  $X(t)$  satisfies (6).

**Theorem 2.** The unique solution for the initial value problem (6) is  $X \in C^*[0, \tau^*]$ .

**Proof:** Given the fractional calculus's inherent features, the equation in (6) may be expressed as

$$I^{1-\vartheta} \frac{d}{dt} X(t) = B_1 X(t) + S(t) B_2 X(t) + I(t) B_3 X(t) + V.$$

Operating by  $I^\vartheta$  we achieve

$$X(t) = X(0) + I^\vartheta (B_1 X(t) + S(t) B_2 X(t) + I(t) B_3 X(t) + V). \tag{7}$$

Let us now  $F: C^*[0, \tau^*] \rightarrow C^*[0, \tau^*]$  described by

$$FX(t) = X(0) + I^\vartheta (B_1 X(t) + S(t) B_2 X(t) + I(t) B_3 X(t) + V). \tag{8}$$

Then

$$\begin{aligned} e^{-Nt} \|FX - FY\| &= e^{-Nt} I^\vartheta \left( B_1(X(t) - Y(t)) + S(t) B_2(X(t) - Y(t)) + I(t) B_3(X(t) - Y(t)) \right) \\ &\leq \left| \frac{1}{\Gamma(\vartheta)} \int_0^t (t-s)^{\vartheta-1} e^{-N(t-s)} (X(s) - Y(s)) e^{-Ns} ds \right| (B_1 + pB_2 + rB_3) \\ &\leq (B_1 + pB_2 + rB_3) \left| \frac{1}{\Gamma(\vartheta)} \int_0^t (u)^{\vartheta-1} e^{-N(u)} \right| \|X - Y\| \\ &\leq \frac{(B_1 + pB_2 + rB_3) \left| \frac{\gamma(\vartheta, Nt)}{\Gamma(\vartheta)} \right|}{N^\vartheta} \|X - Y\|, \end{aligned}$$

where  $\gamma(\vartheta, Nt)$  is the lower incomplete gamma function and  $u = t - s$ . Since  $N$  is an arbitrary, we accept that

$N^\vartheta \geq B_1 + pB_2 + rB_3$ , then we get  $\|FX - FY\| \leq \|X - Y\|$ . Operator  $F$  in (8) has a fixed point. As a result, (7) has a unique solution,  $X \in C^*[0, \tau^*]$ .

In (7), we have

$$\begin{aligned} X(t) &= X(0) + \frac{t^\vartheta}{\Gamma(\vartheta + 1)} (B_1 X(0) + S(0) B_2 X(0) + I(0) B_3 X(0)) \\ &\quad + I^{\vartheta+1} (B_1 X'(t) + S'(t) B_2 X(t) + S(t) B_2 X'(t) + I'(t) B_3 X(t) + I(t) B_3 X'(t)). \end{aligned}$$

$$e^{-Nt}X'(t) = e^{-Nt} \frac{t^\vartheta}{\Gamma(\vartheta)} (B_1X(0) + S(0)B_2X(0) + I(0)B_3X(0) + V) \\ + I^\vartheta (B_1X'(t) + S'(t)B_2X(t) + S(t)B_2X'(t) + I'(t)B_3X(t) + I(t)B_3X'(t)).$$

The assumption  $X' \in C_\delta^*[0, \tau^*]$ . From (7) we have

$$\frac{dX(t)}{dt} = \frac{d}{dt} I^\vartheta (B_1X(t) + S(t)B_2X(t) + I(t)B_3X(t) + V).$$

Operating by  $I^{1-\vartheta}$  we get

$$I^{1-\vartheta} \frac{dX(t)}{dt} = I^{1-\vartheta} \frac{d}{dt} I^\vartheta (B_1X(t) + S(t)B_2X(t) + I(t)B_3X(t) + V).$$

$$D^\vartheta X(t) = (B_1X(t) + S(t)B_2X(t) + I(t)B_3X(t) + V),$$

and

$$X(0) = X_0 + I^\vartheta (B_1X(t) + S(t)B_2X(t) + I(t)B_3X(t) + V).$$

As a result, IVP (6) and Equation (7) are equal.

### 5. Equilibria and Their Stabilities:

The formula for system (5) to determine the equilibrium points is:

$$\Lambda - \beta_1 \frac{S(t)I(t)}{N} - \mu S(t) = 0, \\ \beta_1 \frac{S(t)I(t)}{N} - \mu I(t) - \alpha_2 I(t) - \alpha_3 I(t) = 0, \tag{9}$$

$$\alpha_2 I(t) - \mu R(t) = 0.$$

We achieve the equilibrium point after simplification, where

$$S = \frac{N(\mu + \alpha_2 + \alpha_3)}{\beta_1}, \\ I = \frac{(-N\mu^2 - N\mu\alpha_2 - N\mu\alpha_3 + \Lambda\beta_1)}{(\mu\beta_1 + \alpha_2\beta_1 + \alpha_3\beta_1)}, \\ R = \frac{-\alpha_2(N\mu^2 + N\mu\alpha_2 + N\mu\alpha_3 - \Lambda\beta_1)}{\mu^2\beta_1 + \mu\alpha_2\beta_1 + \mu\alpha_3\beta_1},$$

Then the equilibrium points are:

$$E_1 = \left( \frac{\Lambda}{\mu}, 0, 0 \right), \\ E_2 = \left( \frac{N(\mu + \alpha_2 + \alpha_3)}{\beta_1}, \frac{-N\mu^2 - N\mu\alpha_2 - N\mu\alpha_3 + \Lambda\beta_1}{\mu\beta_1 + \alpha_2\beta_1 + \alpha_3\beta_1}, \frac{-\alpha_2(N\mu^2 + N\mu\alpha_2 + N\mu\alpha_3 - \Lambda\beta_1)}{\mu^2\beta_1 + \mu\alpha_2\beta_1 + \mu\alpha_3\beta_1} \right).$$

**Theorem 3.** Let  $E_1$  be the equilibrium points of model (5). Assume that  $\beta_1 \frac{\Lambda}{\mu N} < \mu + \alpha_2 + \alpha_3$ . Then  $E_1$  is locally asymptotically stable.

**Proof.** The Jacobian matrix of model (5) evaluated at equilibrium point  $E_1$  is given by

$$J(E_1) = \begin{pmatrix} -\mu & -\beta_1 \frac{\Lambda}{\mu N} & 0 \\ 0 & \beta_1 \frac{\Lambda}{\mu N} - \mu - \alpha_2 - \alpha_3 & 0 \\ 0 & \alpha_2 & -\mu \end{pmatrix}$$

According to the characteristic equation  $|J(E_1) - \lambda I| = 0$ .

$$(-\mu - \lambda) \left[ \left( \beta_1 \frac{\Lambda}{\mu N} - \mu - \alpha_2 - \alpha_3 \right) (-\mu - \lambda) \right] = 0,$$

Eigenvalues of  $J(E_1)$  are:

$$\lambda_1 = \beta_1 \frac{\Lambda}{\mu N} - \mu - \alpha_2 - \alpha_3,$$

$$\lambda_{2,3} = -\mu.$$

$$\lambda_i < 0, |\arg(\lambda_i)| = \pi > \frac{\vartheta\pi}{2}, i = 1, 2, 3.$$

According to Theorem 1, equilibrium point is  $E_1$  locally asymptotically stable.

**Theorem 4.** The endemic equilibrium  $E_2$  of the model (5) is asymptotically stable if

$$A_2 = \mu^2 + \mu\alpha_2 + \mu\alpha_3 - \frac{\Lambda\beta_1}{N} > 0.$$

**Proof.** The following is the jacobian matrix for model (5):

$$J(E_2) = \begin{pmatrix} \frac{-\beta_1 \left( \frac{-N\mu^2 - N\mu\alpha_2 - N\mu\alpha_3 + \Lambda\beta_1}{\mu\beta_1 + \alpha_2\beta_1 + \alpha_3\beta_1} \right) - \mu}{N} & \frac{-\beta_1 \left( \frac{N(\mu + \alpha_2 + \alpha_3)}{\beta_1} \right)}{N} & 0 \\ \frac{\beta_1 \left( \frac{-N\mu^2 - N\mu\alpha_2 - N\mu\alpha_3 + \Lambda\beta_1}{\mu\beta_1 + \alpha_2\beta_1 + \alpha_3\beta_1} \right) - \mu}{N} & \frac{\beta_1 \left( \frac{N(\mu + \alpha_2 + \alpha_3)}{\beta_1} \right)}{N} - \mu - \alpha_2 - \alpha_3 & 0 \\ 0 & \alpha_2 & -\mu \end{pmatrix}$$

According to the characteristic equation  $|J(E_2) - \lambda I| = 0$ ,

$$(-\mu - \lambda) \left[ (-\lambda) \left( \frac{-\Lambda\beta_1}{N(\mu + \alpha_2 + \alpha_3)} - \lambda \right) - \left( -\mu + \frac{\Lambda\beta_1}{N(\mu + \alpha_2 + \alpha_3)} \right) (\mu + \alpha_2 + \alpha_3) \right] = 0,$$

we get

$$P(\lambda) = (-\lambda) \left( \frac{-\Lambda\beta_1}{N(\mu + \alpha_2 + \alpha_3)} + \lambda^2 - (-\mu^2 - \mu\alpha_2 - \mu\alpha_3 + \frac{\Lambda\beta_1}{N}) \right) = 0,$$

$$\lambda^2 + \lambda \frac{(\Lambda\beta_1)}{N(\mu + \alpha_2 + \alpha_3)} + \mu^2 + \mu\alpha_2 + \mu\alpha_3 - \frac{\Lambda\beta_1}{N} = 0,$$

where



$$A_1 = \frac{\Lambda\beta_1}{N(\mu + \alpha_2 + \alpha_3)} > 0,$$

$$A_2 = \mu^2 + \mu\alpha_2 + \mu\alpha_3 - \frac{\Lambda\beta_1}{N} > 0.$$

Depending on the Routh-Hurwitz criteria, if  $A_1 > 0$ ,  $A_2 > 0$  hold, we can say that  $E_2$  is asymptotically stable.

### 6. Positivity and Boundedness

**Lemma 1.** (Generalized Mean Value Theorem).

The assumption  $w(t) \in C[a, b]$  and  ${}_0^C D_t^\vartheta w(t) \in C[a, b]$  for  $0 < \vartheta \leq 1$ , then

$$w(t) = w(a) + \frac{1}{\Gamma(\vartheta)} {}_0^C D_t^\vartheta w(\tau)(t - a)^\vartheta,$$

where  $0 \leq \tau \leq t, \forall t \in (a, b]$ .

**Remark 1.** If  $w \in C[0, b]$  and  ${}_0^C D_t^\vartheta (w(t)) \geq 0, \forall t \in (0, b]$ , then the function  $w(t)$  is non-increasing for all  $t \in [0, b]$ .

**Theorem 5.** The solution of model (5) along with initial settings is bounded in  $\mathcal{R}_+^3$ .

**Proof:** Noting that  $\mathcal{R}_+^3$  is positivity invariant, the non negative region.

We obtain from system (5)

$$D^\vartheta S(t)_{S=0} = \Lambda \geq 0,$$

$$D^\vartheta I(t)_{I=0} = 0 \geq 0, \tag{10}$$

$$D^\vartheta R(t)_{R=0} = \alpha_2 I \geq 0.$$

According to system (10) and Remark 1, the solution of model (5) cannot escape from the hyperplanes

$S = 0, I = 0, R = 0$ . if  $(S(0), I(0), R(0)) \in \mathcal{R}_+^3$ . This means that the region  $\mathcal{R}_+^3$  is a collection of positive invariants.

**Theorem 6.**

The region  $P = \{S(t), I(t), R(t) \in \mathcal{R}_+^3, 0 < S(t) + I(t) + R(t) \leq \frac{\Lambda}{\mu}\}$  is an invariant set that is positive for the system

(5).

**Proof.** From model (5) we have

$$D^\vartheta N(t) = \Lambda - \mu(S + I + R) - \alpha_3 I. \text{ This gives that } D^\vartheta N(t) = \Lambda - \mu N(t) - \alpha_3 I.$$

When we apply the Laplace Transform to the previous equation, we have

$$S^\vartheta w(s) - S^{\vartheta-1} N(0) \leq \frac{\Lambda}{S} - \mu w(s),$$

this further provides

$$w(s) \leq \frac{S^{-1}\Lambda}{S^\vartheta + \mu} + \frac{S^{\vartheta-1}N(0)}{(S^\vartheta + \mu)}.$$

From Definitions 3,4,we can infer if  $S_0, I_0, R_0 \in \mathcal{R}_+^3$ , then

$$\begin{aligned} N(t) &\leq \Lambda t^\vartheta E_{\vartheta, \vartheta+1}(-\mu t^\vartheta) + E_{\vartheta, 1}(-\mu t^\vartheta)N(0) \\ &\leq \frac{\Lambda}{\mu} \left( t^\vartheta \mu E_{\vartheta, \vartheta+1}(-\mu t^\vartheta) \right) + E_{\vartheta, 1}(-\mu t^\vartheta) \leq \frac{\Lambda}{\mu} \frac{1}{\Gamma(1)} = \frac{\Lambda}{\mu}. \end{aligned}$$

This indicates that because  $N(t)$  is bounded,  $S(t), I(t),$ and  $R(t)$ , are also bounded.

### 7. Numerical Scheme

We use the Caputo fractional operator to look into the dynamics of the suggested fractional order model (5). The Adams type estimator-corrector method [34–37] is employed to offer the numerical simulation of the proposed nonlinear fractional order system.

Regarding the order  $\vartheta$  Caputo operator, the following Cauchy-type ODE is considered:

$${}^c_0 D_t^\vartheta \phi(t) = \phi(t, \phi(t)), \quad \phi^{(b)}(0) = \phi_0^b, \quad 0 < \vartheta < 1, \quad 0 < t \leq \tau, \tag{11}$$

where  $b = 0, 1, \dots, n - 1$ , and  $n = [\vartheta]$ . Eq. (11) can be turned to the Volterra equation:

$$\phi(t) = \sum_{b=0}^{n-1} \phi_0^{(b)} \frac{t^b}{b!} + \frac{1}{\Gamma(\vartheta)} \int_0^t (t-s)^{\vartheta-1} \phi(s, \phi(s)) ds. \tag{12}$$

By taking into account the numerical solutions of the suggested model using this proposed predictor-corrector scheme connected to the Adam-Bashforth-Moulton algorithm [35], we can take  $h = \tau/N, t_z = zh$ , and  $z = 0, 1, \dots, N \in \mathbb{Z}^+$ , by letting  $\phi_z \approx \phi(t_z)$ , it may be discretized using the associated corrector formula [38], which is as follows:

$$\begin{aligned} S_{q+1} &= \sum_{z=0}^{q-1} S_0^{(z)} \frac{t_{q+1}^z}{z!} + \frac{h^\vartheta}{\Gamma(\vartheta + 2)} \sum_{z=0}^q (p_{z, q+1}) \left( \Lambda - \beta_1 \frac{S_z I_z}{N} - \mu S_z \right) \\ &\quad + \frac{h^\vartheta}{\Gamma(\vartheta + 2)} \sum_{z=0}^q (p_{q+1, q+1}) \left( \Lambda - \beta_1 \frac{S_{q+1}^{PF} I_{q+1}^{PF}}{N} - \mu S_{q+1}^{PF} \right), \\ I_{q+1} &= \sum_{z=0}^{q-1} I_0^{(z)} \frac{t_{q+1}^z}{z!} + \frac{h^\vartheta}{\Gamma(\vartheta + 2)} \sum_{z=0}^q (p_{z, q+1}) \left( \beta_1 \frac{S_z I_z}{N} - \mu I_z - \alpha_2 I_z - \alpha_3 I_z \right) \\ &\quad + \frac{h^\vartheta}{\Gamma(\vartheta + 2)} \sum_{z=0}^q (p_{q+1, q+1}) \left( \beta_1 \frac{S_z I_z}{N} - \mu I_z - \alpha_2 I_z - \alpha_3 I_z \right), \\ R_{q+1} &= \sum_{z=0}^{q-1} R_0^{(z)} \frac{t_{q+1}^z}{z!} + \frac{h^\vartheta}{\Gamma(\vartheta + 2)} \sum_{z=0}^q (p_{z, q+1}) (\alpha_2 I_z - \mu R_z) \\ &\quad + \frac{h^\vartheta}{\Gamma(\vartheta + 2)} \sum_{z=0}^q (p_{q+1, q+1}) (\alpha_2 I_{q+1}^{PF} - \mu R_{q+1}^{PF}), \end{aligned}$$

where

$$S_{q+1}^{PF} = \sum_{z=0}^{q-1} S_0^{(z)} \frac{t_{q+1}^z}{z!} + \frac{h^\vartheta}{\Gamma(\vartheta + 1)} \sum_{z=0}^q (j_{z, q+1}) \left( \Lambda - \beta_1 \frac{S_z I_z}{N} - \mu S_z \right),$$

$$I_{q+1}^{PF} = \sum_{z=0}^{q-1} I_0^{(z)} \frac{t_{q+1}^z}{z!} + \frac{h^\vartheta}{\Gamma(\vartheta + 1)} \sum_{z=0}^q (j_{z,q+1}) \left( \beta_1 \frac{S_z I_z}{N} - \mu I_z - \alpha_2 I_z - \alpha_3 I_z \right),$$

$$R_{q+1}^{PF} = \sum_{z=0}^{q-1} R_0^{(z)} \frac{t_{q+1}^z}{z!} + \frac{h^\vartheta}{\Gamma(\vartheta + 1)} \sum_{z=0}^q (j_{z,q+1}) (\alpha_2 I_z - \mu R_z),$$

and

$$p_{z,q+1} = \begin{cases} q^{\vartheta+1} - (q - \vartheta)(q + 1)^\vartheta, & \text{if } z = 0, \\ (q - z + 2)^{\vartheta+1} + (q - z)^{\vartheta+1} - 2(q - z + 1)^{\vartheta+1}, & \text{if } 1 \leq z \leq q, \\ 1, & \text{if } z = q + 1, \end{cases} \tag{13}$$

where

$$j_{z,q+1} = (q + 1 - z)^\vartheta - (q - z)^\vartheta.$$

### 8. Numeric Simulation

The Adams-Bashforth-Moulton Predictor-Corrector approach is used within this part to display the numerical solution of our model (5) for the values in Table 1. This disease's spread and how certain factors will influence its development have been looked at. Due to this, using the values presented in Table 1, the fluctuation of each subgroup over time is shown for various values of  $\vartheta$ .

In Fig.1, illustrates the susceptible people for various  $\vartheta$  levels to show the most important fractional order. Thus, we can see that the susceptible people decrease over time and after the 10th day, the decrease slows down and becomes almost constant after a certain period of time.

In Fig. 2, we can see that rotavirus-infected individuals noticed the most important fractional order for various values of  $\vartheta$ . As a result, we can see that people infected with rotavirus manifest as a declining course up to about day 10 and an almost constant behaviour for decreasing values of  $\vartheta$ . It is obvious that people infected with rotavirus show this behavior.

In Fig. 3, shows people recovering for various  $\vartheta$  values to most meaningfully see fractional order. Thus, we can observe that the recovered individuals exhibit a behavior that increases over time until the 10th day, and decreases over time for decreasing  $\vartheta$  values, and then the decrease slows down. We can also see that these  $\vartheta$  values intersect between the 20th and 30th days.

In Fig. 4, examines the time-dependent variation of the population in susceptible individuals for different values of  $\beta_1 = 0.3637, \beta_1 = 0.45, \beta_1 = 0.55$  and  $\beta_1 = 0.65$ , which is the transmission coefficient of the disease in the (5) model. Here,  $\beta_1$  value for the real data is taken as  $\beta_1 = 0.3637$ . According to this value, it is observed that the number of susceptible individuals increases over time compared to other values of  $\beta_1$  in the simulation. We are trying to observe the changes in the  $S$  class compared to  $\beta_1$ . The  $S$  class is shown to decline as  $\beta_1$  increases, which is the case. After the 10th day, this decrease slows down and exhibits a nearly constant behavior over time.

In Fig. 5, examines the time-dependent variation of the population of rotavirus-infected individuals for different values of  $\beta_1 = 0.3637, \beta_1 = 0.45, \beta_1 = 0.55$  and  $\beta_1 = 0.65$  of the disease transmission coefficient  $\beta_1$ . It is seen that the number of individuals infected with rotavirus for the value of  $\beta_1 = 0.3637$  is less than the other values of  $\beta_1$  (0.45,0.55,0.65) and the number of individuals infected with rotavirus becomes more stable over time. It is observed that the number of individuals infected with rotavirus is also significantly less for the value of  $\beta_1 = 0.3637$  compared to other values and approaches zero at the end of the simulation period. When we observe the changes

in Class  $I$  compared to  $\beta_1$ , we see that with the increase in  $\beta_1$ , a decrease occurs first in class  $I$ . We then observe that there is an almost constant behavior.

In Fig. 6, changes have been observed in the  $R$  class compared to  $\beta_1$ . With the increase in  $\beta_1$ , we see that the individuals in the  $R$  class, who recovered, showed an increasing attitude until the 10th day, then decreased, then the decrease slowed down.

The numerical values of system (5) are presented in Fig.1-6 for different values of parameter  $\beta_1$  and fractional order  $\vartheta$ . For

$\Lambda = 2.2996e+03, \mu = 0.03360802290, \alpha_2 = 0.008841, \alpha_3 = 0.024, \beta_1 = 0.3736$ , the corresponding equilibrium are:

$$E_2 = (266.7921155, 4.27079087, 1.123483586)$$

In Figures 1-3, we consider the variation in susceptible individuals, infected individuals, and recovered individuals around the equilibrium point  $E_2$  over time for different  $\vartheta$  values. These figures confirm the equilibrium point stability. So theorem 4 is valid. It was concluded that as  $\vartheta$  decreased, susceptible individuals, infected individuals and recovered individuals increased. In addition, the lower the  $\vartheta$  value, the lower the peak and concentration of susceptible individuals, infected individuals, and recovered individuals. From the figures we see that, when the derivative order according to 1-3 is lowered from  $\vartheta = 1$ , the memory effect of the system increases and therefore equilibrium point take longer to be stable. Using the same parameter values above, we consider different  $\beta_1$  values such as  $\beta_1=0.3637, \beta_1=0.45, \beta_1=0.55, \beta_1=0.65$  in Figures 4-6. The corresponding equilibrium points are:

$$E_2 = (266.7921155, 4.27079087, 1.123483586), \beta_1 = 0.3637,$$

$$E_2 = (221.496743, 24.3450718, 7.150003939), \beta_1 = 0.45,$$

$$E_2 = (181.2246079, 47.5483987, 12.50818989), \beta_1 = 0.55,$$

$$E_2 = (153.343899, 61.63921838, 16.21769624), \beta_1 = 0.65.$$

It is seen that as  $\beta_1$  increases, susceptible and recovering individuals decrease, while infected individuals first increase and then decrease. It is easy to see that the local asymptotic stability occurs with respect to the equilibrium point  $E_2$ . These graphs show that model (5) satisfies theorem 4. The biological existence conditions of the equilibrium points are given in Table 1.

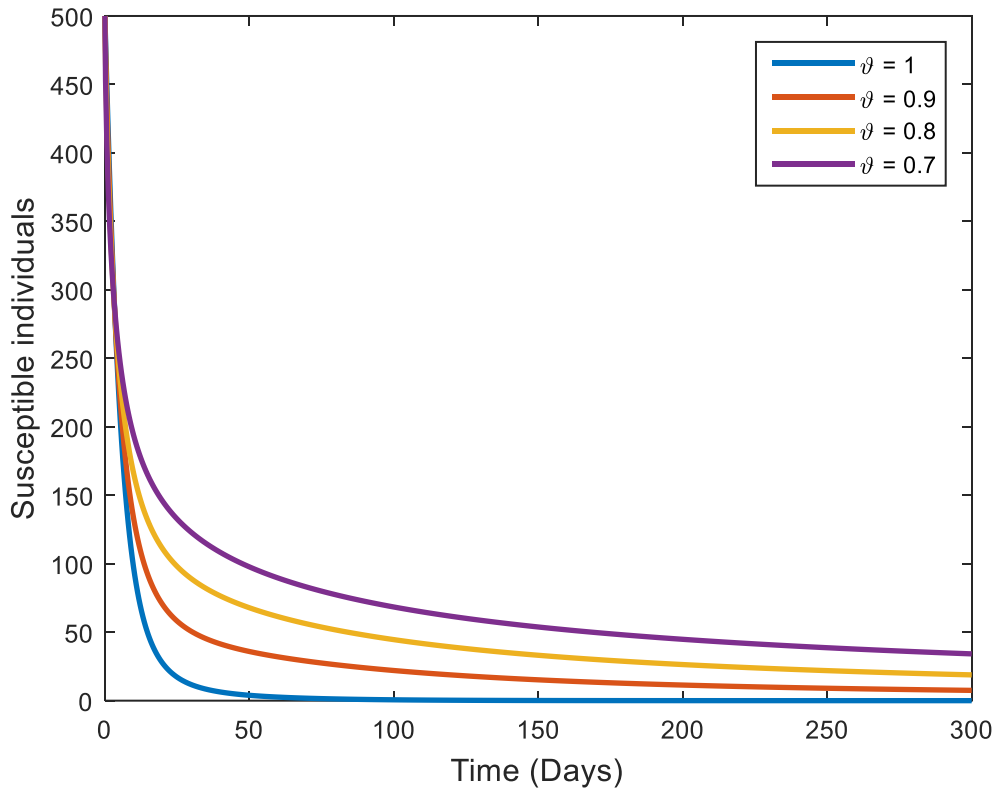


Fig.1.Change of susceptible individuals over time for various fractional order derivatives

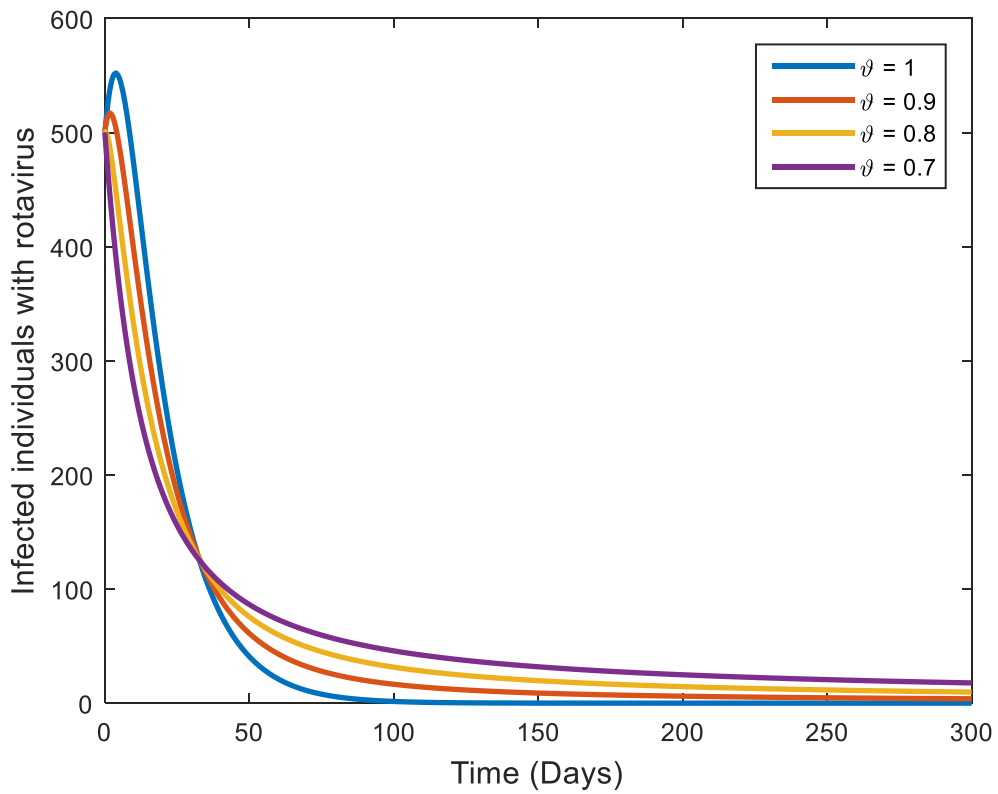


Fig.2.Change of rotavirus-infected individuals over time for various fractional order derivatives.

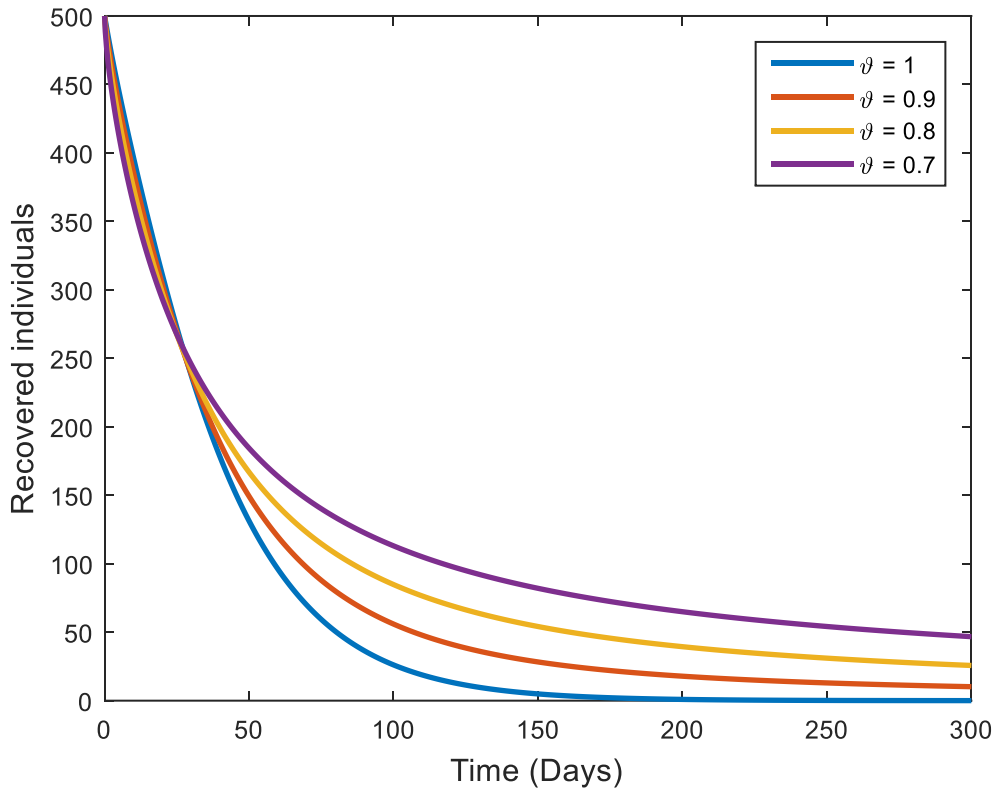


Fig.3. Change of recovered individuals over time for various fractional order derivatives

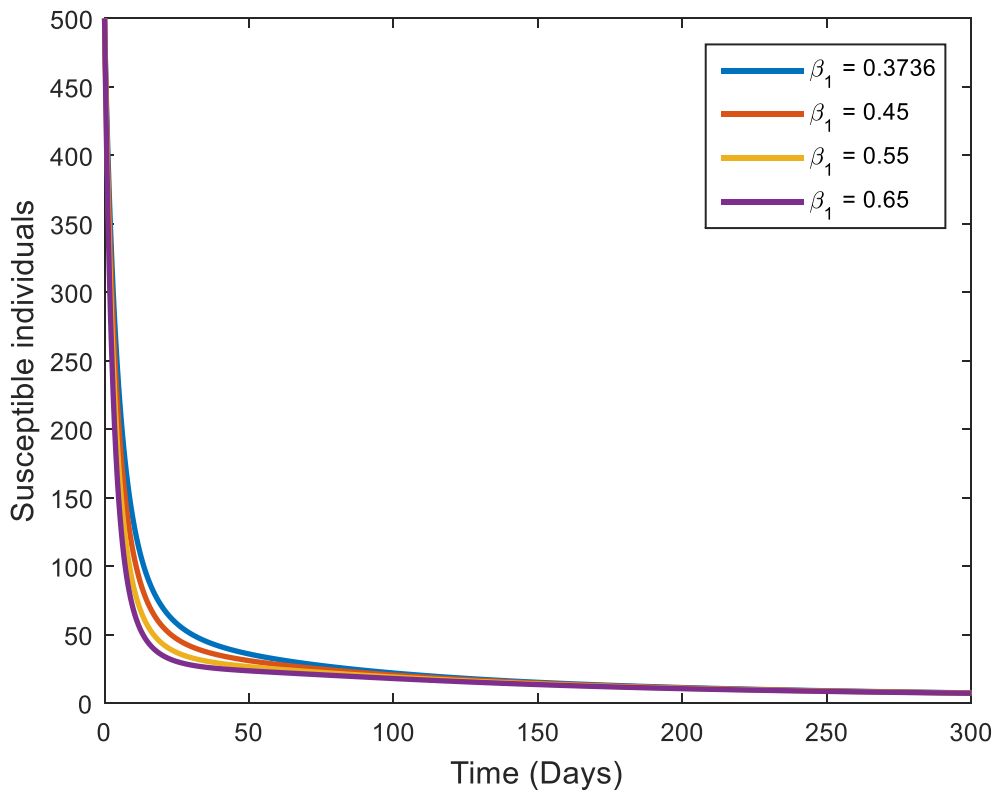


Fig.4. Change of the susceptible individuals over time for the various  $\beta_1$  values and  $\vartheta=0.9$

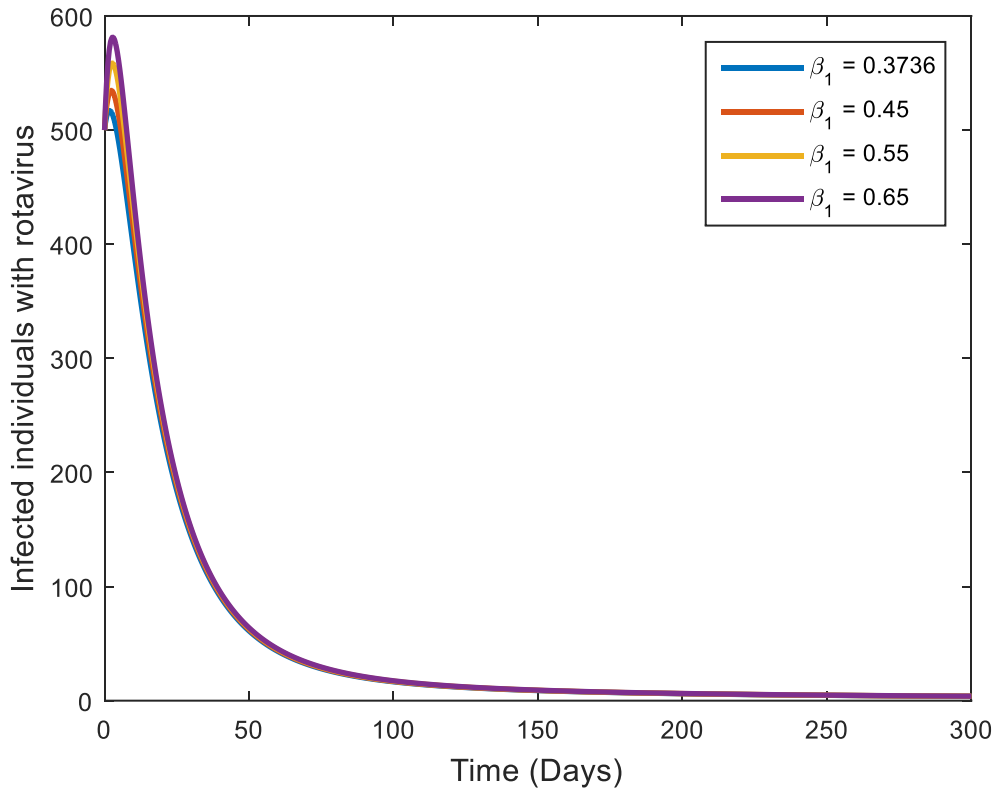


Fig.5. Change of the infected individuals with rotavirus over time for the various  $\beta_1$  values and  $\vartheta=0.9$

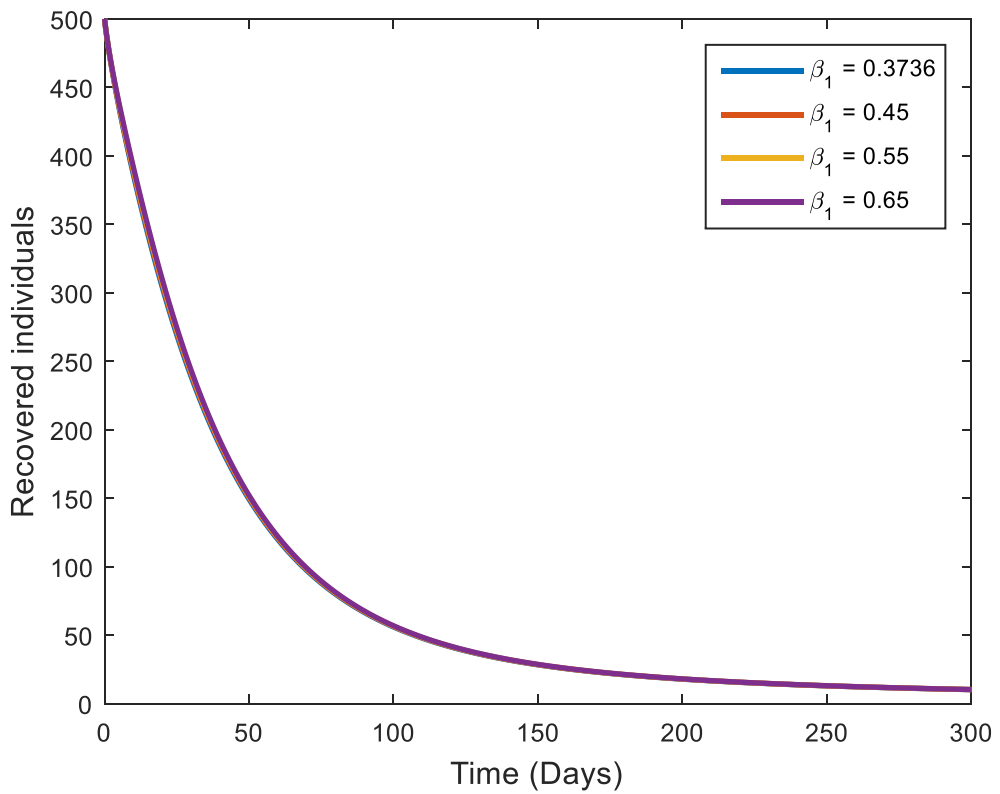


Fig.6. Change of the recovered individuals over time for the various  $\beta_1$  values and  $\vartheta=0.9$

## 9. Discussion and Conclusion

In this paper, first of all, we have given a brief information about rotavirus. Researchers have looked at how rotavirus spreads among people and what effect it has on people. Thus, a new Caputo fractional order mathematical model of disease has been created.

It has been attempted to demonstrate that the system has an equilibrium point and a solution using the fixed point theorem. The system's equilibrium points are located in order to look at the stability of these places. The Adams Bashforth-Moulton approach is used to demonstrate numerical simulations of our concept. The disease model is graphically have been expressed for different parameter values.

For these various parameter values, a difference in the number of rotavirus cases has been noted. It has been estimated that human deaths from this disease will decrease as the rotavirus cases decrease in the future. In addition, it is predicted that the spread of the disease will decrease when the disease transmission coefficient decreases. As may be inferred from the data, this demonstrates that fractional-order equations can be used to more effectively explain the impact of rotavirus.

The model is constructed using fractional-order differential equations. By examining the dynamic behavior of this model, it has been proven that the positive equilibrium point is asymptotic. The graphs for different fractional values of  $\vartheta$  are examined. It has been determined that partial differential equations are more advantageous for mathematical models than full differential equations. The outcomes of the created simulations demonstrate that while the equilibrium points of fractional-order equations and integer order equations are identical, the fractional-order equation solutions take longer to reach the equilibrium point when the  $\vartheta$  parameter drops.

In this way, we hope that the number of people caught and died from rotavirus will decrease significantly by making necessary predictions with the help of these mathematical models and taking necessary precautions and precautions in the future.

### Acknowledgment

The authors thank the referees who contributed to the correction and development of this article.



## References

- [1] Parashar, U. D., Hummelman, E. G., Bresee, J. S., Miller, M. A., & Glass, R. I. 2003. Global illness and deaths caused by rotavirus disease in children. *Emerging infectious diseases*, 9(5), 565.
- [2] Clark, H. F., Glass, R. I., & Offitt, P. A. 1999. Rotavirus vaccines. In plotkin SA, Orenstein WA (eds). *Vaccines*.
- [3] Collins, P. L., McIntosh, K., & Chanock, R. M. 1996. Respiratory syncytial virus In: Fields BN, Knipe DM, Howley PM, et al.(eds) *Fields Virology*.
- [4] Parashar, U. D., Gibson, C. J., Bresee, J. S., & Glass, R. I. 2006. Rotavirus and severe childhood diarrhea. *Emerging infectious diseases*, 12(2), 304.
- [5] Liu, L., Johnson, H. L., Cousens, S., Perin, J., Scott, S., Lawn, J. E., ... & Black, R. E. 2012. Global, regional, and national causes of child mortality: an updated systematic analysis for 2010 with time trends since 2000. *The lancet*, 379(9832), 2151-2161.
- [6] Bozdayi, G., Dogan, B., Dalgic, B., Bostanci, I., Sari, S., Battaloglu, N. O., ... & Ahmed, K. 2008. Diversity of human rotavirus G9 among children in Turkey. *Journal of medical virology*, 80(4), 733-740.
- [7] Kurugol, Z., Geylani, S., Karaca, Y., Umay, F., Erensoy, S., Vardar, F., ... & Ozkinay, C. 2003. Rotavirus gastroenteritis among children under five years of age in Izmir, Turkey. *Turkish Journal of Pediatrics*, 45(4), 290-294.
- [8] Cataloluk, O., Iturriza, M., & Gray, J. 2005. Molecular characterization of rotaviruses circulating in the population in Turkey. *Epidemiology & Infection*, 133(4), 673-678.
- [9] Ceyhan, M., Alhan, E., Salman, N., Kurugol, Z., Yildirim, I., Celik, U., ... & Pawinski, R. 2009. Multicenter prospective study on the burden of rotavirus gastroenteritis in Turkey, 2005–2006: a hospital-based study. *The Journal of infectious diseases*, 200(Supplement\_1), S234-S238.
- [10] Kurugöl, Z., & Salman, N. 2008. Rotavirus infeksiyonları ve aşılar. *Ankem Dergisi*, 22(3), 160-170.
- [11] Santos, N., & Hoshino, Y. 2005. Global distribution of rotavirus serotypes/genotypes and its implication for the development and implementation of an effective rotavirus vaccine. *Reviews in medical virology*, 15(1), 29-56.
- [12] Mızrakçı, S. 2022. Rotavirus konulu yayınlara global bakış. *Black Sea Journal of Health Science*, 5(2), 239-244.
- [13] Aydın, E., Aydın, N., & Perçin Renders, D. U. Y. G. U. 2022. Evaluation of the Effect of Acute Gastroenteritis Factors on Laboratory Parameters in Pediatric Patients. *Flora Enfeksiyon Hastalıkları Ve Klinik Mikrobiyoloji Dergisi*, 27(1).
- [14] Dalir, M., & Bashour, M. 2010. Applications of fractional calculus. *Applied Mathematical Sciences*, 4(21), 1021-1032.
- [15] Loverro, A. 2004. Fractional calculus: history, definitions and applications for the engineer. *Rapport technique*, Univeristy of Notre Dame: Department of Aerospace and Mechanical Engineering, 1-28.
- [16] Podlubny, 1999. *I. Fractional differential equations*, Academic Pres, New York.
- [17] Oldham, K.B.; Spanier, 1974. *J. The fractional calculus*, Academic Pres, New York.
- [18] Miller, K.S.; Ross, B. 1993. *An introduction to the fractional calculus and fractional differential equations*, Wiley, New York.
- [19] Hilfer, 2000. *R. Applications of fractional calculus in physics*, World Scientific, Singapore.
- [20] Öztürk, I., & Özköse, F. 2020. Stability analysis of fractional order mathematical model of tumor-immune system interaction. *Chaos, Solitons & Fractals*, 133, 109614.
- [21] Naik, P. A., Zu, J., & Owolabi, K. M. 2020. Global dynamics of a fractional order model for the transmission of HIV epidemic with optimal control. *Chaos, Solitons & Fractals*, 138, 109826.
- [22] Özköse, F., Şenel, M. T., & Habbireeh, R. 2021. Fractional-order mathematical modelling of cancer cells-cancer stem cells-immune system interaction with chemotherapy. *Mathematical Modelling and Numerical Simulation with Applications*, 1(2), 67-83.
- [23] Özköse, F., Habbireeh, R., & Şenel, M. T. 2023. A novel fractional order model of SARS-CoV-2 and Cholera disease with real data. *Journal of Computational and Applied Mathematics*, 423, 114969.
- [24] Yavuz, M., Özköse, F., Susam, M., & Kalidass, M. 2023. A new modeling of fractional-order and sensitivity analysis for hepatitis-b disease with real data. *Fractal and Fractional*, 7(2), 165.
- [25] Sabbar, Y., Yavuz, M., & Özköse, F. 2022. Infection Eradication Criterion in a General Epidemic Model with Logistic Growth, Quarantine Strategy, MediaIntrusion, and Quadratic Perturbation. *Mathematics*, 10(22), 4213.
- [26] Sene, N. 2022. Theory and applications of new fractional-order chaotic system under Caputo operator. *An International Journal of Optimization and Control*, 12(1), 20-38.
- [27] Evirgen, F., Esmehan, U. Ç. A. R., Sümeýra, U. Ç. A. R., & Özdemir, N. 2023. Modelling influenza a disease dynamics under Caputo-Fabrizio fractional derivative with distinct contact rates. *Mathematical Modelling and Numerical Simulation with Applications*, 3(1), 58-72.

- [28] Veerasha, P., Yavuz, M., & Baishya, C. 2021. A computational approach for shallow water forced Korteweg–De Vries equation on critical flow over a hole with three fractional operators. *An International Journal of Optimization and Control: Theories & Applications (IJOCTA)*, 11(3), 52-67.
- [29] Odionyenma, U. B., Ikenna, N., & Bolaji, B. 2023. Analysis of a model to control the co-dynamics of Chlamydia and Gonorrhoea using Caputo fractional derivative. *Mathematical Modelling and Numerical Simulation with Applications*, 3(2), 111-140.
- [30] Atede, A. O., Omame, A., & Inyama, S. C. 2023. A fractional order vaccination model for COVID-19 incorporating environmental transmission: a case study using Nigerian data. *Bulletin of Biomathematics*, 1(1), 78-110.
- [31] NWAJERĪ, U. K., ATEDE, A. O., PANLE, A. B., & EGEONU, K. U. 2023. Malaria and cholera co-dynamic model analysis furnished with fractional-order differential equations. *Mathematical Modelling and Numerical Simulation with Applications*, 3(1), 33-57.
- [32] Özköse, F., Yavuz, M., Şenel, M. T., & Habbireeh, R. 2022. Fractional order modelling of omicron SARS-CoV-2 variant containing heart attack effect using real data from the United Kingdom. *Chaos, Solitons & Fractals*, 157, 111954.
- [33] Özköse, F., & Yavuz, M. 2022. Investigation of interactions between COVID-19 and diabetes with hereditary traits using real data: A case study in Turkey. *Computers in biology and medicine*, 141, 105044.
- [34] Diethelm, K., & Freed, A. D. 1998. The FracPECE subroutine for the numerical solution of differential equations of fractional order. *Forschung und wissenschaftliches Rechnen*, 1999, 57-71.
- [35] Diethelm, K. 1997. An algorithm for the numerical solution of differential equations of fractional order. *Electronic transactions on numerical analysis*, 5(1), 1-6.
- [36] Garrappa, R. 2010. On linear stability of predictor–corrector algorithms for fractional differential equations. *International Journal of Computer Mathematics*, 87(10), 2281-2290.
- [37] Garrappa, R. 2018. Numerical solution of fractional differential equations: A survey and a software tutorial. *Mathematics*, 6(2), 16.
- [38] Li C, Tao C. 2009. On the fractional adams method. *Comput Math Appl*, 58(8):1573–88.
- [39] Naik, P. A., Yavuz, M., Qureshi, S., Zu, J., & Townley, S. 2020. Modeling and analysis of COVID-19 epidemics with treatment in fractional derivatives using real data from Pakistan. *The European Physical Journal Plus*, 135, 1-42.
- [40] Özköse, F., Yılmaz, S., Yavuz, M., Öztürk, İ., Şenel, M. T., Bağcı, B. Ş., ... & Önal, Ö. 2022. A fractional modeling of tumor-immune system interaction related to lung cancer with real data. *The European Physical Journal Plus*, 137, 1-28.
- [41] Susam, M. 2022. Hepatit-B Hastalığının Kesirli Mertebeden Matematiksel Modeli ve Türkiye’den Gerçek Veri ile Parametre Tahmini (Master's thesis, Necmettin Erbakan Üniversitesi Fen Bilimleri Enstitüsü).